Single-Crystal EPR Study at 95 GHz of the Type 2 Copper Site of the Inhibitor-Bound Quercetin 2,3-Dioxygenase

Maria Fittipaldi,* Roberto A. Steiner,† Michio Matsushita,‡ Bauke W. Dijkstra,† Edgar J. J. Groenen,* and Martina Huber*

*Department of Molecular Physics, Huygens Laboratory, Leiden University, Leiden, the Netherlands; †Department of Chemistry, Laboratory of Biophysical Chemistry, University of Groningen, Groningen, the Netherlands; and ‡Department of Physics, Tokyo Institute of Technology, Tokyo, Japan

ABSTRACT An electron-spin-echo-detected, electron-paramagnetic-resonance study has been performed on the type 2 copper site of quercetin 2,3-dioxygenase from *Aspergillus japonicus*. In the protein, copper is coordinated by three histidine nitrogens and two sulfurs from the inhibitor diethyldithiocarbamate. A single crystal of the protein was studied at 95 GHz and the complete *g*-tensor determined. The electron-paramagnetic-resonance data are compatible with two orientations of the principal *g*-axes in the copper center, one of which is preferred on the basis of an analysis of the copper coordination and the *d*-orbitals that are involved in the unpaired-electron orbital. For this orientation, the principal *z*-axis of the *g*-tensor makes an angle of 19° with the Cu-N(His112) bond and the *N* of His112 may be considered the axial ligand. The singly occupied molecular orbital contains a linear combination of copper d_{xy} and d_{yz}-orbitals, which are antibonding with atomic orbitals of histidine nitrogens and diethyldithiocarbamate sulfurs. The orientation of the *g*-tensor for the quercetin 2,3-dioxygenase is compared with that for type 1 copper sites.

INTRODUCTION

Copper sites in proteins and enzymes serve various functions. Research nowadays focuses on the relation between (electronic) structure and function. Type 1 copper sites (Peisach and Blumberg, 1974), which are active in electron-transfer reactions, have been extensively studied and correlations between variations in the metal coordination and electronic structure have been elucidated (Solomon et al., 1992). High-field electron-paramagnetic-resonance (EPR) studies on single crystals have given detailed information on the type 1 site in azurin (Coremans et al., 1994), mutants thereof (Coremans et al., 1996; van Gastel et al., 2000), and nitrite reductase (van Gastel et al., 2001).

As yet, less is known about type 2 sites, in particular about those that catalyze biochemical transformations in enzymes. Here we are concerned with the copper site of a quercetin 2,3-dioxygenase (hereafter referred to as 2,3QD) from *Aspergillus japonicus*.

Dioxygenases are enzymes that use molecular oxygen to oxidize their substrates by incorporating both oxygen atoms into the reaction product. These enzymes take part in the biosynthesis and catabolism of different metabolites and in detoxification (Hayaishi, 1974). Specifically, 2,3QD is a copper-containing dioxygenase that catalyzes the oxidation of the flavonol quercetin to 2-protocatechuoylphloroglucinol carboxylic acid with concomitant production of carbon monoxide. It is unusual, since most other dioxygenases employ a non-heme iron. The crystal structure of the 2,3QD from *Aspergillus japonicus* has been recently determined in its free (Fusetti et al., 2002), inhibitor-complexed (Steiner et al., 2002b), and anaerobic substrate-complexed (Steiner et al., 2002a) forms. These structures reveal differences in the geometry of the Cu-sites for the three forms. From X-band EPR studies on frozen solutions of the enzyme, paramagnetic copper was found to be active in all forms of 2,3QD investigated. The *g*-values and hyperfine parameters have been determined and differences between native, substrate-bound, and inhibitor-bound forms were discussed (Kooter et al., 2002).

In the present article, the complete *g*-tensor of the copper site is reported, which has been determined from a 95-GHz high-field EPR study on single crystals of 2,3QD. The enzyme was investigated with the inhibitor diethyldithiocarbamate (DDC) bound to the active site (2,3QD·DDC). The inhibitor-bound form of 2,3QD was chosen, because EPR on frozen solutions of native 2,3QD showed a superposition of two signals (Kooter et al., 2002), owing to differences in ligation deriving from two conformations of the Glu73 (Fusetti et al., 2002). Binding of DDC results in a unique conformation with a single EPR signal. The sulfur coordination and the unusual EPR parameters of the inhibitor-bound form raise specific interest in the electronic structure of that site. In 2,3QD·DDC, copper is coordinated by three histidine nitrogens and two sulfurs from the DDC molecule (Fig. 1) with a geometry that has been described as between trigonal bipyramidal and distorted tetrahedral (Steiner et al., 2002b). The *g*-values of 2,3QD·DDC are close to those of type 1 copper sites, whereas the hyperfine coupling of copper (A_{zz}) is much closer to that expected for a type 2 copper site (Peisach and Blumberg, 1974). As yet

Submitted May 13, 2003, and accepted for publication August 15, 2003.

Address reprint requests to Martina Huber, Dept. of Molecular Physics, Huygens Laboratory, Leiden University, P.O. Box 9504, 2300 RA Leiden, the Netherlands. Tel.: 31-71-527-5560; Fax: 31-71-527-5819; E-mail: mhuber@molphys.leidenuniv.nl.

Roberto A. Steiner's present address is Structural Biology Laboratory, Dept. of Chemistry, University of York, York YO10 5YW, UK.

0006-3495/03/12/4047/08 $2.00

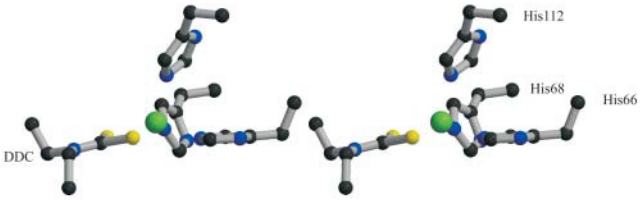

FIGURE 1 Stereo representation of the copper site of 2,3QD·DDC.

little is known about the electronic structure of the copper center and the binding mode of DDC. Here we report the first determination of the *g*-tensor directions for a type 2 copper center in proteins. The observed directions of the principal axes of the *g*-tensor allow a discussion of the copper coordination in 2,3QD·DDC and in particular of the orbital containing the unpaired electron.

MATERIALS AND METHODS

The crystals of 2,3QD·DDC used in the experiment have been obtained as previously described (Steiner et al., 2002b).

Electron-spin-echo (ESE) experiments have been performed using a homebuilt 95-GHz spectrometer (Disselhorst et al., 1995) with a microwave bridge manufactured by the Department of Microwave Equipment for Millimeter Waveband ESR Spectroscopy in Donetsk, Ukraine. The measurements were performed at a temperature of 1.2 K. The single crystal was mounted in a quartz tube with an inner and outer diameter of 0.6 and 0.84 mm, respectively. The tube ends were sealed by wax. The dimensions of the crystal were $0.4 \times 0.1 \times 0.05$ mm^3. A two-pulse microwave excitation sequence with pulse lengths of 140 and 200 ns, respectively, separated by 300 ns, was used at a repetition rate of 5 Hz. The intensity of the echo was recorded as a function of the magnitude of the external magnetic field $\mathbf{B_0}$ in the range 3–3.4 T. All orientations of $\mathbf{B_0}$ with respect to the crystal were measured without remounting the crystal, owing to the capabilities of the spectrometer to rotate the sample and $\mathbf{B_0}$ about orthogonal axes. The cw-EPR measurement on the frozen solution was performed using a 95 GHz ELEXSYS E 680 spectrometer (Bruker, Rheinstetten, Germany).

RESULTS

The ESE-detected EPR spectra

The EPR spectra in Fig. 2 reveal the dependence of the ESE signal on the orientation of the external magnetic field, $\mathbf{B_0}$, with respect to the crystal. The 2,3QD·DDC crystals belong to the space group $P2_1$ with the unit cell containing two asymmetric units with four molecules each. Therefore, the EPR spectrum consists of eight resonances for an arbitrary orientation of $\mathbf{B_0}$ with respect to the crystal. When $\mathbf{B_0}$ is parallel to the principal *x*-axis of the *g*-tensor (g_x) of one molecule, the related resonance becomes stationary at the high-field side of the spectrum, corresponding to the lowest *g*-value (g_{xx}). On the other hand, a resonance becomes stationary at the low-field side of the spectrum (g_{zz}) when $\mathbf{B_0}$ is parallel to the principal *z*-axis of the *g*-tensor (g_z) of one molecule. According to these criteria the orientation of the

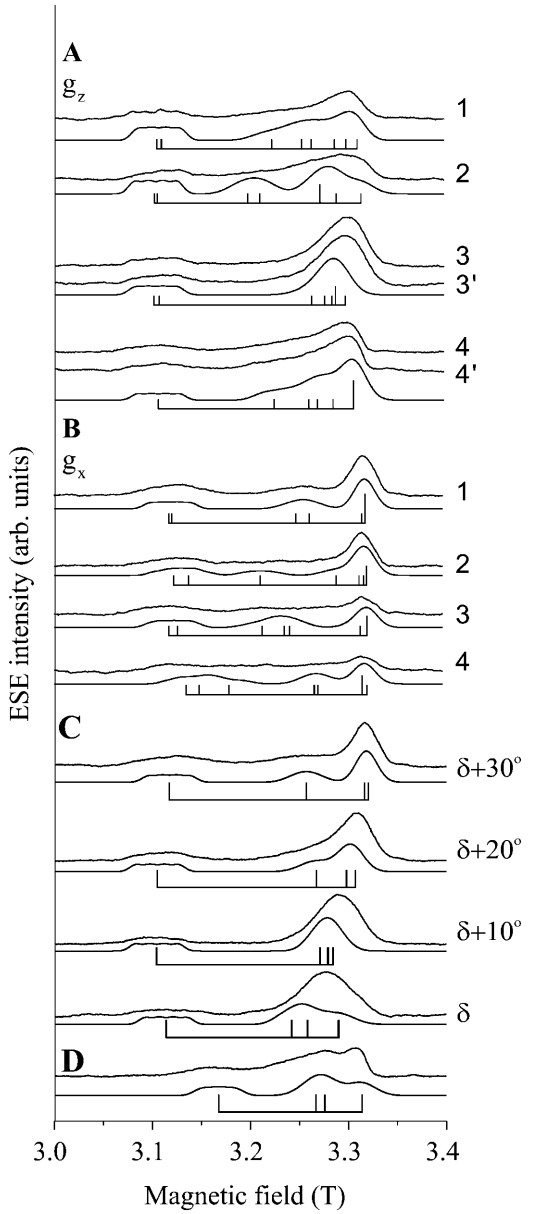

FIGURE 2 ESE-detected EPR spectra (absorption type) at 95 GHz of a single crystal of 2,3QD·DDC for different orientations of the magnetic field with respect to the crystal. (*A*) Spectra 1, 2, 3, and 4 correspond to the orientations of $\mathbf{B_0}$ along the experimentally determined g_z axes of the four distinct molecules. For each orientation an experimental spectrum (*top*), a stick diagram with the calculated line positions (*bottom*), and the stick diagram dressed with Gaussian lines (*middle*), are shown. The stick spectra show that each EPR spectrum derives from eight paramagnetic centers in the unit cell; sticks have been drawn on top of each other when resonances were calculated to be within 3 mT. The spectra 3′ and 4′ are C_2 related to the spectra 3 and 4, respectively. (*B*) Spectra with $\mathbf{B_0}$ along four distinct experimentally determined g_x axes. (*C*) Spectra with $\mathbf{B_0}$ in the plane perpendicular to the C_2 axis taken at successive 10° intervals. (*D*) Spectrum with $\mathbf{B_0}$ parallel to the C_2 axis.

x- and *z*- principal axes of the eight molecules in the unit cell are determined in a laboratory reference frame. For each direction of a g_x axis, a g_z axis is found which is perpendicular to this g_x axis within 4°.

The two asymmetric units in the unit cell are related by a twofold screw axis, whose effect on the EPR spectra is equivalent to that of a C_2 symmetry axis. This implies that the eight spectra along the respective g_x (g_z) axes comprise two groups of four each. For each spectrum in one group there is an equivalent spectrum in the other group (compare to Fig. 2 *A*, spectra 3 and 3′, 4 and 4′). From the symmetry-related pairs, the approximate direction of the C_2 axis is deduced, which, subsequently, is optimized. When $\mathbf{B_0}$ is either parallel or perpendicular to the C_2 axis, the two asymmetric units become magnetically equivalent, which results in four distinct resonances (Fig. 2, *C* and *D*). Spectra have been measured in intervals of 10° with $\mathbf{B_0}$ in the plane perpendicular to the C_2 axis, and in addition ~40 spectra at randomly chosen orientations were acquired. For resonances with $\mathbf{B_0} \parallel g_z$ (Fig. 2 *A*), a hyperfine splitting of 14.7 mT owing to the copper nuclear spin is resolved.

The high-field cw-EPR spectrum of a frozen solution of 2,3QD·DDC is shown in Fig. 3. Simulation of the spectrum yields an estimate of the rhombicity ($g_{yy} - g_{xx} = 0.0045$), and a hyperfine splitting A_{zz} of 14.7 mT in agreement with the value obtained from the single-crystal measurements.

To further characterize the electronic structure, the optical absorption spectrum of 2,3QD·DDC was measured, which reveals a broad absorption band ~400 nm. The molar extinction coefficient (ε) is estimated from the absorbance at 400 nm relative to that at 280 nm using the molar extinction coefficient of the native, monomeric 2,3QD of $\varepsilon = 61455$ cm^{-1} M^{-1} at 280 nm (R. Steiner, personal communication). This results in $\varepsilon = (4850 \pm 850)$ cm^{-1} M^{-1} at 400 nm.

Data analysis

The ESE-detected EPR spectra

The ESE-detected EPR spectra of the single crystal have been simulated to refine the measured directions of the principal axes of the *g*-tensors of the molecules in the unit cell. For a certain direction of $\mathbf{B_0}$ with respect to the crystal, the resonance field for each molecule is given by

$$B_{\text{res}} = \frac{h\nu}{\mu_\beta \left[\sum_i (g_{ii} \cos \phi_i)^2\right]^{1/2}}, \quad i = x, y, z, \qquad (1)$$

where h is Planck's constant, ν is the frequency of the microwave radiation, μ_β is the Bohr magneton, and ϕ_i is the angle between the principal *i*-axis of the *g*-tensor of the molecule and the direction of $\mathbf{B_0}$.

The g_{xx} and g_{zz} values of 2.0406 and 2.1868 were obtained from the resonances at the extreme field values of the single-crystal ESE spectra. For g_{yy} a value of 2.0461 was used, which is slightly larger than that derived from the frozen solution spectrum. Owing to the large linewidth in the field region where g_{xx} and g_{yy} contribute most, the simulations were not very sensitive to the magnitude of g_{yy} and the larger value provided the best description of the single-crystal measurements. The resonance fields calculated from Eq. 1 were fit to all observed EPR spectra, those for $\mathbf{B_0}$ along the *x*- and *z*-principal axes, for $\mathbf{B_0}$ in the plane perpendicular to the C_2 axis, and for the randomly chosen orientations of $\mathbf{B_0}$ with respect to the crystal. The ϕ_i angles, which reflect the directions of the principal axes, were optimized in a nonlinear least-squares fit constrained by the symmetry of the space group and by the orthogonality requirements. In Fig. 2, the resonance fields of the eight molecules in the unit cell, calculated on the basis of the optimized orientation of the *g*-tensor principal axes, are shown as stick spectra. Lineshape simulations were performed by dressing the stick spectra with Gaussians, using an anisotropic linewidth model (Coremans et al., 1994). The hyperfine coupling of copper along the *z*-direction of the *g*-tensor (A_{zz}) of 14.7 mT was included explicitly.

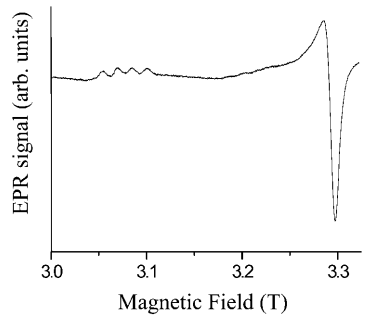

FIGURE 3 Continuous wave (derivative type) EPR spectrum at 95 GHz of a frozen solution of 2,3QD·DDC. Temperature 40 K, modulation amplitude 1.2 mT, modulation frequency 100 kHz, and microwave power 5 μW.

Above 3.25 T, the spectra comprise a large number of close-lying resonances, which are not resolved in the experimental spectra. Consequently, the uncertainty in the directions of the g_x and g_y axes is larger than for the g_z axis. The refined directions for g_x are within 20° of the directions determined in the experiments and for g_z within 10°. The resultant directions of the *g* principal axes are shown in a Wulffnet projection (Fig. 4) in the laboratory reference frame ($\mathbf{x_L}$, $\mathbf{y_L}$, and $\mathbf{z_L}$). In Table 1 the direction cosines of the principal axes of the eight g-tensors are given with respect to the same axis system. This laboratory reference frame has been obtained from the frame in which the measurements were performed by a rotation which aligned the $\mathbf{y_L}$ axis with the C_2 symmetry axis, whereas the other two axes ($\mathbf{x_L}$, $\mathbf{z_L}$) were arbitrarily chosen.

Assignment: orientation of the g-tensor axes relative to the copper-ligand directions

One of the goals of the EPR study is to determine the orientation of the principal axes of the *g*-tensor in the copper center. The experiment reveals eight *g*-tensors, which belong to the eight molecules in the unit cell. To find out to which

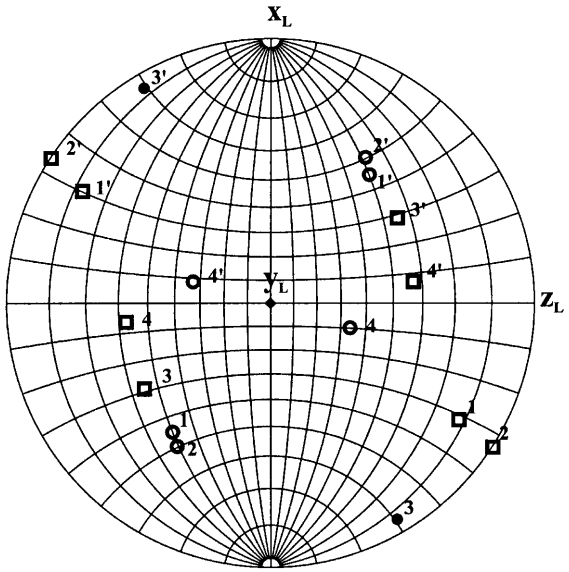

FIGURE 4 Wulffnet projection of the orientations of the g_x and g_z principal axes of the eight g-tensors with respect to the laboratory reference frame $\mathbf{x_L}$, $\mathbf{y_L}$, and $\mathbf{z_L}$. The $\mathbf{y_L}$ axis is parallel to the crystallographic C_2 axis; $\mathbf{x_L}$ and $\mathbf{z_L}$ axes have arbitrary directions. Circles: directions of g_z axes; squares: directions of g_x axes. Primed and unprimed numbers refer to the g-tensors that belong to the molecules in one or the other asymmetric unit. The direction of the C_2 axis is the bisector of any couple of g_x or g_z axes of tensors i-i'. Unfilled symbols refer to vectors pointing below, solid symbols to vectors pointing above the projection plane.

molecule each of the g-tensors has to be assigned, we make use of the structure of the unit cell as determined by x-ray diffraction.

The criterion for a proper assignment is that the orientation of the principal axes of the g-tensor with respect to the copper-ligand directions is the same (within the experimental accuracy) for each molecule in the unit cell. We define the orientation of each molecule in the unit cell by a local Cartesian axis system based upon vectors pointing from the copper toward the N_ε atoms of the His66 and His112 ligands. To couple the laboratory (EPR) axis system and the crystallographic axis system, we align the C_2 axis from the EPR experiments with the crystallographic C_2 axis. The mutual orientation of both axis systems about this C_2 axis has been taken into account explicitly (angle θ) in the further analysis. From the EPR spectra the eight g-tensors are pairwise related by the C_2 axis, which leaves eight ways to choose four out of the eight tensors that may belong to one of the asymmetric units. These four tensors can be coupled to the four molecules in the asymmetric unit in 4! ways. Altogether this corresponds to $8(4!) = 192$ ways to assign the g-tensors to the molecules in the crystallographic unit cell. For each possible assignment, we have calculated for all molecules in the unit cell the orientation of the g-tensors in the local axis systems for all values of θ ($0° < \theta < 360°$ in steps of 1°). The criterion of identical orientation of the g-tensor in the copper center for all molecules in the unit cell is met for two orientations of the g-tensor. In the further analysis we focus on the g_z axis because it is determined more accurately from the experiments than the g_x and g_y axes. For the two possible assignments (I and II), the orientation of the g_z axis in the copper site differs by $<8°$ for the various molecules in the unit cell. Other assignments give rise to variations of at least 22°. The resulting possible orientations of the g_z axis with respect to the copper-ligand directions are represented in Table 2 and illustrated in Fig. 5. For assignment I of the g-tensor, g_z points approximately toward the N_ε of His112. The nitrogens N_ε of His66 and His68 together with the sulfur atoms S(1) and S(2) of the inhibitor are approximately in the plane perpendicular to g_z. For assignment II of the g-tensor, g_z points approximately toward the N_ε of His66, whereas the N_ε of His112 and His68 and the S(2) are approximately in the plane perpendicular to g_z.

DISCUSSION

The complete g-tensor of the paramagnetic copper center in 2,3QD·DDC has been obtained from single crystal W-band EPR spectroscopy. The analysis yields the assignment of the measured g-tensors to the eight crystallographic sites and allows two distinct assignments (I and II) of the g-tensor principal axes in the copper site. Here we discuss the electronic structure of the copper site on the basis of the g-tensor and meanwhile try to discriminate between these possibilities. The stationary fields of resonance yielded a first

TABLE 1 Refined directions of the principal axes (g_x, g_y, and g_z) of the g-tensors

		$g1$	$g2$	$g3$	$g4$	$g1'$	$g2'$	$g3'$	$g4'$
	x	−0.5133	−0.5475	−0.4826	−0.1059	0.5130	0.5470	0.4825	0.1068
g_x	y	−0.2046	−0.0093	−0.5101	−0.5311	−0.2045	−0.0090	−0.5101	−0.5312
	z	0.8334	0.8367	−0.7117	−0.8399	−0.8338	−0.8366	0.7123	0.8404
	x	−0.4902	−0.3449	0.1810	0.9794	0.4907	0.3451	−0.1814	−0.9788
g_y	y	0.8667	0.9132	−0.8537	−0.2028	0.8666	0.9129	−0.8531	−0.2024
	z	−0.0898	−0.2155	0.4880	0.0044	0.0895	0.2161	−0.4883	−0.0036
	x	−0.7045	−0.7630	−0.8565	−0.1720	0.7045	0.7623	0.8572	0.1725
g_z	y	−0.4551	−0.4071	0.1062	−0.8222	−0.4549	−0.4069	0.1069	−0.8225
	z	−0.5446	−0.5030	0.5042	0.5417	0.5449	0.5034	−0.5041	−0.5418

For each axis, the direction cosines are specified in the laboratory reference frame $\mathbf{x_L}$, $\mathbf{y_L}$, and $\mathbf{z_L}$, of which $\mathbf{y_L}$ coincides with the crystallographic C_2 axis. The eight g-tensors correspond to the eight molecules in the unit cell, g_i' is related to g_i by the C_2 axis.

TABLE 2 Angles between the g_z axis and the copper-ligand directions or the normal to copper-ligand planes for assignments I and II

	g_z (I)	g_z (II)
Cu-N66	69°	17°
Cu-N68	83°	98°
Cu-N112	19°	107°
Cu-S(1)	107°	123°
Cu-S(2)	106°	78°
N66-Cu-N68	22°	
N112-Cu-N68		23°
S(1)-C-S(2)	15°	48°

estimate of the directions of the g-tensor principal axes. During refinement through simulation of the EPR spectra for many orientations of the magnetic field with respect to the crystal, the initial directions changed at most by 20° for the g_x and 10° for the g_z axes. The larger corrections for g_x reflect the larger uncertainty of the g_x direction, which is caused by the near-axial symmetry of the g-tensor and the large linewidth and spectral overlap in the field region where these signals are observed in the single-crystal EPR spectra. In the Discussion we therefore focus on the direction of the g_z axes.

Electronic structure of the copper site from the *g*-tensor

We analyze the tensor directions to determine the nature of the orbital that contains the unpaired electron (SOMO). From the fact that the tensor is close to axially symmetric and that g_{zz} is larger than g_{xx} and g_{yy}, we conclude that the SOMO on copper contains the d_{xy} rather than the d_{z^2}-orbital (Wertz and Bolton, 1986). For a pure d_{xy}-orbital, the direction of g_z is normal to the plane of the maximum probability amplitude of the d-orbital, hereafter referred to as the plane of the d_{xy}-orbital. Ligands providing orbitals that overlap with this d-orbital can be identified from their orientation relative to g_z.

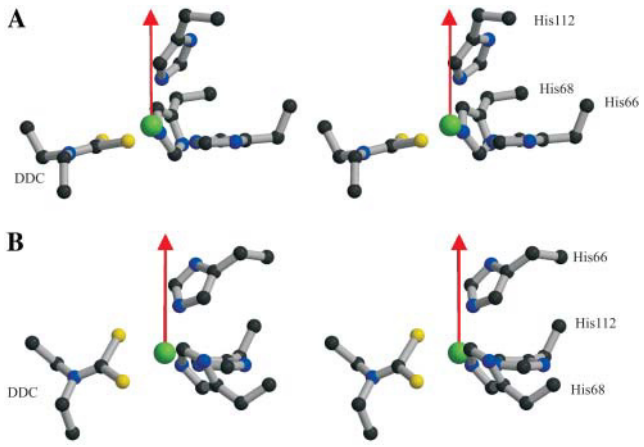

FIGURE 5 Stereo representation of the orientation of g_z in the copper site (*A*) for assignment I, (*B*) for assignment II.

In Table 2 the angles between the g_z axis and the copper ligand bonds are listed. Axial ligands are expected to be close to the g_z direction. For assignment I of the g-tensor, the angle between g_z and the Cu-N(His112) direction is small, for assignment II the angle between g_z and the Cu-N(His66) direction is small. The short Cu-N distances (Table 3) for these histidines imply a strong axial ligand. For both assignments, the angles between the Cu-N directions of the other two histidines and g_z are ~90°. For assignment I, these concern His66 and His68; for assignment II, these concern His112 and His68. The Cu-N directions of each pair of histidines make an angle of ~90° (Table 3). Thus, for both g-tensor assignments, the geometry is ideal for σ-overlap of the nitrogen lone pair orbitals of the histidines with the d_{xy}-orbital. The d-orbitals are defined with respect to the following coordinate system. The N-Cu-N plane (assignment I: the N66-Cu-N68 plane; assignment II: N112-Cu-N68 plane) is the X,Y-plane and Z (Z^{I} and Z^{II}, respectively) is the direction normal to that plane. The X-axis (X^{I} and X^{II}, respectively) bisects the Cu-N directions of the histidines in the X,Y-plane. In this coordinate system the angle of g_z with respect to the Z-axes is 22° for I and 23° for II. The tilt angle of g_z with respect to the Z-axis indicates that the SOMO is not a pure d_{xy}-orbital, but a linear combination with other d-orbitals. Since the tilt angles with respect to Z for assignments II and I are the same within experimental accuracy, these do not enable us to discriminate between the two possible assignments of the g-tensor in the copper site.

Besides the histidine nitrogens, copper is ligated by the sulfur atoms of the DDC molecule. One sulfur atom (S1) is significantly closer to the copper than the other (see Table 3), but both are within coordinating distance. DDC has a delocalized π-electron system, involving p_π-orbitals at both sulfur atoms and the carbon atom they are bound to. In

TABLE 3 Copper-ligand distances and ligand-copper-ligand angles from the crystal structure (PDB code 1GQG); see Steiner et al. (2002b)

	Distances (Å)
Cu-N(His66)	2.15 (0.06)
Cu-N(His68)	2.10 (0.05)
Cu-N(His112)	2.15 (0.02)
Cu-S1	2.24 (0.07)
Cu-S2	2.88 (0.07)
	Angles (degrees)
N66-Cu-N68	92 (3)
N66-Cu-N112	91 (2)
N68-Cu-N112	105 (1)
N66-Cu-S1	139 (4)
N66-Cu-S2	90 (3)
N68-Cu-S1	99 (2)
N68-Cu-S2	155 (2)
N112-Cu-S1	123 (2)
N112-Cu-S2	100 (2)

The values are the average values of the four molecules in the asymmetric unit. The standard deviation is given in parentheses.

first approximation, the symmetry axes of the p_π-orbitals of the sulfurs are thus perpendicular to the S-C-S plane, whereas the lone-pair orbitals of the sulfurs are in the S-C-S plane. Although rehybridization at the sulfur to increase overlap with the metal-centered orbitals may occur, the binding of both sulfurs to the copper cannot be considered independent from the orientation of the S-C-S plane.

For assignment I, the *X,Y*-plane concerns the N66-Cu-N68 plane, and the two sulfur atoms are on the same side of this plane. The angle between the S-C-S plane and the N-Cu-N plane is 36°. With respect to the coordinate system defining the *d*-orbitals, the normal to the S-Cu-S plane makes an angle of 81° with Y^I, i.e., it is almost in the *X,Z*-plane (Table 4). Thus, the S-Cu-S plane is related to the N-Cu-N plane by a rotation almost about the Y^I-axis. Bonding of copper to the sulfur atoms in this case involves a linear combination of the d_{xy}-orbital and the d_{yz}-orbital, since the latter orbital is related to the d_{xy}-orbital by a rotation about the *Y*-axis. The contribution to the *g*-tensor from the copper *d*-electrons in the orbital resulting from this linear combination would be axial, as observed, and g_z would have an orientation in between the directions of the normals to the N-Cu-N plane and the S-C-S plane (van Gastel et al., 2000). This applies to assignment I, as reflected in the small angles of g_z with respect to the normals to both planes (Table 2), and by the fact that the angle between g_z and the Y^I-axis is within experimental uncertainty identical to that of the normal to the S-Cu-S plane and that axis (Table 4).

For assignment II, the *X,Y*-plane concerns the N112-Cu-N68 plane. Of the sulfurs, S(2) is close to this plane (angle N66-Cu-S(2) = 90°) and the Cu-S bond is oriented such that its lone-pair orbital overlaps with the d_{xy}-orbital (angle N112-Cu-S(2) = 100°). The large distance of S(2) to Cu, however, makes this interaction weak. Consequently, the sulfur character of the SOMO will be small and the direction of the g_z axis is expected to be close to perpendicular to the d_{xy} (N112-Cu-N68) plane, which is not observed. The optical absorption spectrum, and the magnitude of the *g*-values (see below) suggest that the sulfur atoms contribute substantially to the SOMO, therefore, the *g*-tensor assignment I is the more likely one, and the one we consider below.

Comparison with type 1 copper sites

Among the copper sites in proteins, the type 1 copper sites are the best-characterized (Solomon et al., 1992). The orientation of the *g*-tensor has been measured for several of such sites (Coremans et al., 1994, 1996; van Gastel et al., 2000, 2001), and a model to correlate the electronic structure with the *g*-tensor directions has been proposed (van Gastel et al., 2001). This model was supported by recent ab initio quantum-chemical calculations of the *g*-tensor of azurin (van Gastel et al., 2002). Structurally, blue type 1 sites have a trigonal coordination with three in-plane ligands, two histidine nitrogens, and a cysteine sulfur. In most cases the axial ligand is a weak ligand. The orientation of the dominant copper *d*-orbital in the SOMO is determined by the antibonding overlap with the lone-pair orbitals of the nitrogens, and, consequently, the direction of g_z is virtually perpendicular to the N-Cu-N plane.

TABLE 4 Angles defining orientation of the normal to the S-Cu-S plane and the g_z axis for assignments I and II in the *d*-orbital reference frame

		X	*Y*	*Z*
I	Normal to S-Cu-S	51°	81°	40°
	g_z axis	70°	80°	22°
II	Normal to S-Cu-S	117°	138°	60°
	g_z axis	112°	95°	23°

The rhombicity of the *g*-tensor is small and derives at least partly from spin-orbit coupling at the sulfur (Penfield et al., 1985; van Gastel et al., 2002). On the other hand, for a more strongly bound axial ligand, the d_{z^2}-orbital might take part in the SOMO. Analysis reveals that a small contribution of this orbital to the SOMO already results in a substantial rhombicity of the *g*-tensor (Gewirth et al., 1987; De Kerpel et al., 1998; Coremans et al., 1996; van Gastel et al., 2000). The copper-hyperfine interaction is commonly small for type-1 copper sites (Peisach and Blumberg, 1974).

Compared with azurin, which has the copper site closest to ideally trigonal of all known blue-copper proteins, four observations from the EPR study on 2,3QD·DDC deserve attention. First, the orientation of the g_z axis deviates significantly (22°) from the normal to the plane spanned by the equatorial nitrogens and the copper (1° for azurin). Secondly, the g_{zz} value of 2,3QD·DDC (2.1868) is substantially smaller than for azurin (2.273). Thirdly, the rhombicity ($g_{yy} - g_{xx}$) of the *g*-tensor is even smaller than for azurin (0.0055 vs. 0.017). Fourthly, the *z*-component of the copper hyperfine interaction for 2,3QD·DDC (450 MHz) is about twice that for azurin (229 MHz).

The orthogonality of the g_z direction with respect to the N-Cu-N plane for the blue-copper sites results from the fact that the d_{xy}-orbital combines σ -(antibonding) overlap with the lone pair orbitals of the nitrogens with π (antibonding) overlap with the sulfur p_y-orbital. If the sulfur participates in the SOMO but is no longer (about) in the N-Cu-N plane, σ-overlap with the sulfur should take over which requires participation of another copper *d*-orbital in the SOMO (LaCroix et al., 1996; Pierloot et al., 1998; van Gastel et al., 2001). This changes the orientation of the g_z axis. The observed orientation for 2,3QD·DDC in combination with the negligibly small rhombicity argues in favor of the linear combination of d_{xy} and d_{yz} of copper *d*-orbitals in the SOMO, which represents antibonding interaction with both histidine nitrogens and the DDC sulfur atomic orbitals.

The deviation of g_{zz} from the free-electron *g*-value is determined by spin-orbit coupling. In a perturbative treatment, this deviation derives from the spin-orbit-coupling-induced mixing of excited states into the ground state, which

depends on the excited-state wavefunctions and excitation energies. As yet no quantum-chemical description is available for 2,3QD·DDC and any conclusion should be considered with caution. Ab initio calculations on a model copper site of azurin show that the g_{zz} value is most sensitive to the spin-density distribution between copper and its ligands (van Gastel et al., 2002). The smaller g_{zz} value for 2,3QD·DDC might suggest a spin density in the copper *d*-orbitals smaller than for azurin. On the other hand, the excitation energies for the relevant excited states may be higher for 2,3QD·DDC than for azurin (as found for the intense transition in the visible region of the spectrum), but as yet knowledge on the low-energy excited states of 2,3QD·DDC in the infrared, where the relevant transitions are expected, is lacking.

Despite the strongly bound axial ligand, the rhombicity of the *g*-tensor in 2,3QD·DDC is small. We conclude that the contribution of the d_{z^2}-orbital to the SOMO must be negligibly small. We further note that, although delocalization of the wave function onto sulfur is required, for example to explain the direction of the g_z axis, in contrast to azurin, the contribution of spin-orbit coupling on sulfur does not seem to lead to substantial rhombicity in the case of 2,3QD·DDC. In view of the difference in electronic structure between the sites of azurin and 2,3QD·DDC, the interpretation of the changes in spin density responsible for the difference in the A_{zz} values of both sites requires quantum-mechanical calculations, which will be performed in the future.

Optical absorption

The extinction coefficient of 2,3QD·DDC is similar to that of the blue copper sites of azurin (628 nm, $\varepsilon = 5700\ \mathrm{cm}^{-1}\ \mathrm{M}^{-1}$), but the transition of 2,3QD·DDC is at a higher energy than in azurin. In type 1 copper sites, optical absorption in this range has been associated with delocalization of the wave function onto the sulfur, suggesting that in the case of 2,3QD·DDC, interaction with the sulfur is also important. The shorter wavelength of the absorption could be an indication for the more strongly bonding, respectively antibonding, character of the molecular orbitals. Larger excitation energies might be (partly) responsible for the smaller g_{zz} value for 2,3QD·DDC compared to azurin.

Summary

In summary, the complete *g*-tensor of the type 2 site of 2,3QD·DDC has been determined. The *z*-axis of the *g*-tensor makes an angle of 19° with the Cu-N(His112) bond and the *N* of His112 may be considered the axial ligand. The qualitative interpretation presented in this article shows that the knowledge of the direction of the principal axes of the *g*-tensor allows an analysis of the electronic structure of the copper site. A quantitative description will be possible by ab initio quantum-chemical calculation of the *g*-tensor. Single-crystal high-field EPR studies on the catalytically active site of the substrate-bound 2,3QD are planned.

We thank Dr. L. Bubacco for contributions early in the project and Dr. M. van Gastel for help in the analysis of the experimental data. We are indebted to Prof. G.W. Canters for support and many helpful discussions.

The work in Leiden was performed under the auspices of the BIOMAC research school of Leiden and Delft Universities. R.A.S. acknowledges support by the Netherlands Foundation for Chemical Research and financial aid from the Netherlands Organization for Scientific Research.

REFERENCES

Coremans, J. W. A., O. G. Poluektov, E. J. J. Groenen, G. W. Canters, H. Nar, and A. Messerschmidt. 1994. A W-band electron-paramagnetic-resonance study of a single-crystal of azurin. *J. Am. Chem. Soc.* 116:3097–3101.

Coremans, J. W. A., O. G. Poluektov, E. J. J. Groenen, G. C. M. Warmerdam, G. W. Canters, H. Nar, and A. Messerschmidt. 1996. The azurin mutant Met121Gln: a blue-copper protein with a strong axial ligand. *J. Phys. Chem.* 100:19706–19713.

De Kerpel, J. O. A., K. Pierloot, U. Ryde, and B. O. Roos. 1998. Theoretical study of the structural and spectroscopic properties of stellacyanin. *J. Phys. Chem. B.* 102:4638–4647.

Disselhorst, J. A. J. M., H. van der Meer, O. G. Poluektov, and J. Schmidt. 1995. A pulsed EPR and ENDOR spectrometer operating at 95 GHz. *J. Magn. Reson. A.* 115:183–188.

Fusetti, F., K. H. Schroter, R. A. Steiner, P. I. van Noort, T. Pijning, H. J. Rozeboom, K. H. Kalk, M. R. Egmond, and B. W. Dijkstra. 2002. Crystal structure of the copper-containing quercetin 2,3-dioxygenase from *Aspergillus japonicus*. *Structure*. 10:259–268.

Gewirth, A. A., S. L. Cohen, H. J. Schugar, and E. I. Solomon. 1987. Spectroscopic and theoretical studies of the unusual EPR parameters of distorted tetrahedral cupric sites: correlations to x-ray spectral features of core levels. *Inorg. Chem.* 26:1133–1146.

Hayaishi, O. 1974. Molecular Mechanism of Oxygen Activation. Academic Press, New York.

Kooter, I. M., R. A. Steiner, B. W. Dijkstra, P. I. van Noort, M. R. Egmond, and M. Huber. 2002. EPR characterization of the mononuclear Cu-containing *Aspergillus japonicus* quercetin 2,3-dioxygenase reveals dramatic changes upon anaerobic binding of substrates. *Eur. J. Biochem.* 269:2971–2979.

LaCroix, L. B., S. E. Shadle, Y. N. Wang, B. A. Averill, B. Hedman, K. O. Hodgson, and E. I. Solomon. 1996. Electronic structure of the perturbed blue copper site in nitrite reductase: spectroscopic properties, bonding, and implications for the entatic/rack state. *J. Am. Chem. Soc.* 118:7755–7768.

Peisach, J., and W. E. Blumberg. 1974. Structural implications derived from the analysis of the electron paramagnetic resonance spectra of natural and artificial copper proteins. *Arch. Biochem. Biophys.* 165: 691–708.

Penfield, K. W., A. A. Gewirth, and E. I. Solomon. 1985. Electronic structure and bonding of the blue copper site in plastocyanin. *J. Am. Chem. Soc.* 107:4519–4529.

Pierloot, K., J. O. A. De Kerpel, U. Ryde, M. H. M. Olsson, and B. O. Roos. 1998. Relation between the structure and spectroscopic properties of blue copper proteins. *J. Am. Chem. Soc.* 120:13156–13166.

Solomon, E. I., M. J. Baldwin, and M. D. Lowery. 1992. Electronic structures of active sites in copper proteins: contributions to reactivity. *Chem. Rev.* 92:521–542.

Steiner, R. A., K. H. Kalk, and B. W. Dijkstra. 2002a. Anaerobic enzyme-substrate structures provide insight into the reaction mechanism of the

copper-dependent quercetin 2,3-dioxygenase. *Proc. Natl. Acad. Sci. USA*. 99:16625–16630.

Steiner, R. A., I. M. Kooter, and B. W. Dijkstra. 2002b. Functional analysis of the copper-dependent quercetin 2,3-dioxygenase. 1. Ligand-induced coordination changes probed by x-ray crystallography: inhibition, ordering effect, and mechanistic insights. *Biochemistry*. 41:7955–7962.

van Gastel, M., M. J. Boulanger, G. W. Canters, M. Huber, M. E. P. Murphy, M. P. Verbeet, and E. J. J. Groenen. 2001. A single-crystal electron paramagnetic resonance study at 95 GHz of the type 1 copper site of the green nitrite reductase of *Alcaligenes faecalis*. *J. Phys. Chem. B*. 105:2236–2243.

van Gastel, M., G. W. Canters, H. Krupka, A. Messerschmidt, E. C. de Waal, G. C. M. Warmerdam, and E. J. J. Groenen. 2000. Axial ligation in blue-copper proteins. A W-band electron spin echo detected electron paramagnetic resonance study of the azurin mutant M121H. *J. Am. Chem. Soc*. 122:2322–2328.

van Gastel, M., J. W. A. Coremans, H. Sommerdijk, M. C. van Hemert, and E. J. J. Groenen. 2002. An ab initio quantum-chemical study of the blue-copper site of azurin. *J. Am. Chem. Soc*. 124:2035–2041.

Wertz, J. E., and J. R. Bolton. 1986. Electron Spin Resonance. Chapman & Hall, New York.